

Thermally Activated Exciton Dissociation and Recombination Control the Organometal Halide Perovskite Carrier Dynamics

Tom J. Savenije,¹ Carlito S. Ponseca, Jr.,² Lucas Kunneman¹, Mohamed Abdellah,² Kaibo Zheng,² Yuxi Tian,² Qiushi Zhu,³ Sophie E. Canton,³ Ivan Scheblykin,² Tonu Pullerits,² Arkady Yartsev,² and Villy Sundström²

¹Optoelectronic Materials Section, Department of Chemical Engineering, Delft University of Technology, Delft, The Netherlands

²Division of Chemical Physics, Lund University, Lund, Sweden

³Department of Synchrotron Radiation Instrumentation, Lund University, Lund, Sweden

Supporting Information

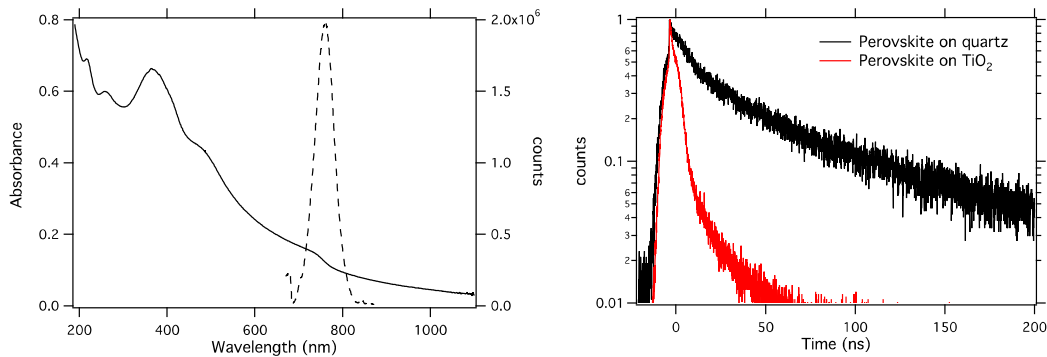


Figure 1S. (left) Steady state absorption (full line) and PL (dashed line) spectrum of $(\text{CH}_3\text{NH}_3)\text{PbI}_3$. (right) Time correlated single photon counting lifetime measurements on $(\text{CH}_3\text{NH}_3)\text{PbI}_3$ on optical excitation at 440 nm with 1.63×10^{11} photons/cm² per pulse. Rep. rate is 400 KHz.

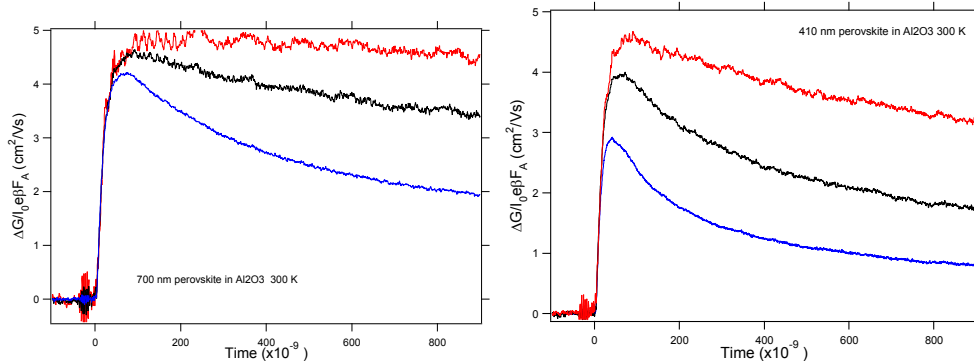


Figure 2S. Comparison between TRMC traces obtained on excitation at 700 nm (left) and at 410 nm (right; identical to those shown in Figure 2 in main text). The TRMC traces are corrected for

their optical attenuation. Most importantly, the initial signal sizes are comparable at the lowest intensities (red lines). The decay kinetics are different due to the fact that the concentration profiles vary, which is caused by differences in the size of the absorption coefficients.

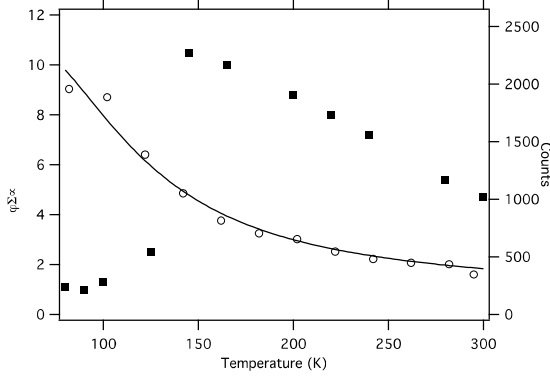


Figure 3S. Dependence of the maximum TRMC signal (squares) versus temperature determined at an incident intensity of ca 5×10^{-9} cm^2 /per pulse. At 145 K a dramatic drop in signal size can be observed. In contrast the PL data (open circles) including the fit as described in the main text show only a gradual change in luminescence with temperature.

Fitting of TRMC transients

The TRMC traces shown in Figure 2 were fitted using a routine based on the mathematical model as detailed in Scheme 1 of the main text. For the calculations the concentrations within the perovskite layers are assumed to be homogeneous. The optical excited states are not explicitly included in the fitting routine. Concentrations are calculated by numerically solving a set of differential equations as given below using Igor Pro.

$$\begin{aligned} \frac{\partial [\text{Per}]}{\partial t} &= -G(t)\phi + \gamma[\text{Per}^+ + e^-] \\ \frac{\partial [\text{Per}^+ + e^-]}{\partial t} &= G(t)\phi - \gamma[\text{Per}^+ + e^-] - k_1[\text{Per}^+ + e^-] + k_2[(\text{Per}^+ + e^-)_{\text{dis}}] \\ \frac{\partial [(\text{Per}^+ + e^-)_{\text{dis}}]}{\partial t} &= k_1[\text{Per}^+ + e^-] - k_2[(\text{Per}^+ + e^-)_{\text{dis}}] \end{aligned}$$

Solving the numerical equations yields the time dependent concentration of $\text{Per}^+ + e^-$ and $(\text{Per}^+ + e^-)_{\text{dis}}$. Next the concentrations curves $\text{Per}^+ + e^-$ and $(\text{Per}^+ + e^-)_{\text{dis}}$ are multiplied with the total charge carrier mobility using Equation 3 given in the main text. Finally, a convolution is applied with an exponential function with a time constant of 18 ns to take into account the instrumental

response of the set-up. The routine optimizes the rates constants to fit all TRMC traces obtained using different intensities with one set of rate constants for each temperature.

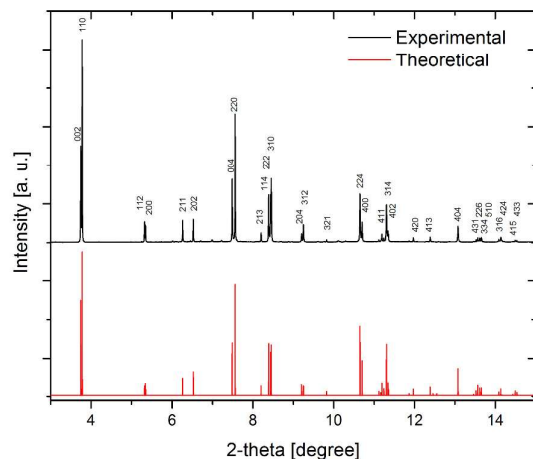


Figure 4S. XRD pattern of $(\text{CH}_3\text{NH}_3)\text{PbI}_3$ powder at room temperature. The experiment was carried out using beam line 11BM, APS, Argonne National Laboratory, US. The X-ray wavelength is 0.4137 angstrom. The $(\text{CH}_3\text{NH}_3)\text{PbI}_3$ is quite pure, and there are no detectable traces of PbI_2 with any possible space group.¹⁻³ The crystal structure of produced perovskite is: crystal system - orthorhombic, space group- $I4cm$, symmetry $Z=16$, obtained by using the program GSAS.^{4,5}

- (1) Wyckoff, R. W. G., New York, Interscience Publishers: *Crystal Structures* **1963**, 239.
- (2) Palosz, B.; Steurer, W.; Schulz, H. *J. Phys.: Cond. Matter*, **1990**, 2, 5285.
- (3) Mitchell, R.S. *Z. Kristallogr.* **1959**, 111, 372@C384.
- (4) Larson, A.C.; Von Dreele, R.B. General Structure Analysis System (GSAS), Los Alamos National Laboratory Report LAUR, **2000** 86-748.
- (5) B. H. Toby, EXPGUI, A graphical user interface for GSAS, *J. Appl. Cryst.* **2001**, 34, 210-213.